Carbon Letters (2023) 33:177–190
https://doi.org/10.1007/s42823-022-00415-w

Online ISSN 2233-4998
Print ISSN 1976-4251

ORIGINAL ARTICLE

A facile ultrasound-assisted synthesis of mesoporous carbon

Rayanne O. Araujo[1] · Vanuza O. Santos[1] · Jamily L. Santos[1] · Flaviana C. P. Ribeiro[1] · Maria J. F. Costa[2] · Jamal S. Chaar[1] · Newton P. S. Falcão[3] · Carlos E. F. da Costa[4] · Luiz K. C. de Souza[1]

Received: 17 July 2022 / Revised: 23 September 2022 / Accepted: 28 September 2022 / Published online: 6 October 2022

Abstract
The ultrasonic method is an alternative to the conventional route to produce structured carbon materials, offering the advantages of synthesis in a short period of time under room temperature. The main objective of this work is to synthesize a sulfonated mesoporous carbon catalyst from a phenolic resin composed of phloroglucinol and formaldehyde. The synthesis was performed by the soft-template method in an ultrasonic processor and the product was subsequently carbonized and sulfonated for application in the esterification model reaction. Functionalization with sulfuric acid of MCS5-6 h sample brought about a decrease in porosity but simultaneously resulted in the generation of functional groups of an acidic nature. The MCS5-6 h catalyst with a sulfonic density of 1.6 mmol g^{-1}, surface area of 402 m^2 g^{-1} and pore diameter of 10.6 nm maintained in mesoporous even after acid treatment. MCS5-6 h showed excellent activity in the esterification reaction with 95% oleic acid conversion. The recyclability of MCS5-6 h was satisfactory during five reaction cycles. The present work addressed a promising alternative for the synthesis of carbon catalysts using ultrasound irradiation, thus providing an alternative with a lower cost of time and energy for large-scale production.

Keywords Ultrasonic method · Phenolic resin · Sulfonated mesoporous carbon and esterification

1 Introduction

Mesoporous carbon has advanced physicochemical properties, such as adjustable porosity of the ordered structure, high specific surface area and high chemical, thermal and mechanical stability. This makes it quite versatile in its applications in catalysis, electrochemistry, energy storage, CO_2 capture, water purification and adsorption. Its porosity is essential to guarantee a performance adjusted to the target application. It is controlled through modifications in the synthesis of mesoporous carbon. Thus, new synthesis methods capable of controlling the size/volume of pores accompanied by a low impact on the reduction of the surface area are indispensable [1].

Mesoporous carbon is produced by soft-template or hard-template methods. The latter consists of the preparation of an mesoporous silica mold followed by filling its pores with carbon precursors; after carbonization, the silica mold is removed by treatment with acidic/basic solutions. A disadvantage of this method is the use of expensive templates, which also increase the number of preparation steps, and finally, the use of harsh chemicals in their removal [2]. The soft-template method manufactures mesoporous carbon by exploiting the advantageous interaction of phenolic resins with a targeting agent, which is removed by thermal decomposition. There is a consensus that this synthesis pathway reduces the number of synthesis steps in addition to using a biodegradable targeting agent. This allows control of pore size/volume, easy template elimination and low cost [3].

The conventional route used in the synthesis of mesoporous carbon is the hydrothermal method, which requires high temperatures (above 100 °C), the use of autoclaves and a long preparation time, sometimes up to three days. That is why research is still intense in the search for

✉ Luiz K. C. de Souza
ls@ufam.edu.br

[1] Department of Chemistry, Federal University of Amazonas, Manaus, AM, Brazil

[2] School of Engineering of Sao Carlos, Department of Materials Engineering, University of Sao Paulo, Sao Carlos, SP, Brazil

[3] Coordination of Technology and Innovation, National Institute for Amazon Research, Manaus, AM, Brazil

[4] Department of Chemistry, Federal University of Para, Belem, PA, Brazil

low-cost synthesis paths with reduced environmental risks and low energy consumption that ensure an ordered porous structure.

The ultrasonic method has been suggested as an alternative to produce structured carbon materials, offering the advantages of synthesis in a short period of time under ambient temperature and atmospheric pressure. In this method, the efficiency is dependent on the frequency, intensity of the waves, temperature, type of solvent and pressure applied to the system [4]. By carefully controlling these parameters, the synthesis conditions are optimized by creating new materials with particle sizes and shapes that are adjustable to the target application [2]. Modification in the preparation parameters facilitates the formation of chemical species, including metals, alloys, oxides, sulfides, carbides and catalyst supports.

The ultrasound-assisted production of carbon materials performed by El-Khodary et al. [5] obtained hierarchical 3D porous carbon activated by KOH for application in supercapacitors. Ching et al. [6] also produced high surface area (917 $m^2 g^{-1}$) cellulose in hydrogels for methylene blue removal. Zhang et al. [7] studied the fabrication of gold nanoparticle/carbon nanosheet composites by the sonoelectrochemical method.

This method of preparing carbon materials controls properties such as porosity and the distribution of active sites in catalysts. The control of surface chemistry by functionalization with acid groups improves the interaction between the reactants and the catalyst surface, promoting high performance in catalytic reactions. For example, Tamborini et al. [8] synthesized sulfonated mesoporous carbon for 48 h and obtained a material with a surface area of 140 $m^2 g^{-1}$ and a sulfonic density of 0.39 mmol g^{-1} to esterify 60.6% oleic acid. A similar synthesis time was observed by Dong et al. [9] in the preparation of sulfonated porous carbon with a surface area of 393 $m^2 g^{-1}$ and a sulfonic density of 1.71 mmol g^{-1}.

Although the conventional route is efficient to obtain sulfonated mesoporous carbon catalysts with high surface areas and densities of sulfonic groups, its efficiency is limited by the long preparation time. This work offers the novel synthesis of a sulfonated mesoporous carbon catalyst assisted by ultrasound. The soft-template method was assisted by an ultrasonic processor, producing a heterogeneous catalyst applied in the esterification model reaction. The mesoporous coal obtained here has a high surface area (up to 549 $m^2 g^{-1}$), high pore volume (0.83 $cm^3 g^{-1}$) and uniform pore size distribution (centered at 12.1 nm). The sulfonic groups were highly concentrated, favoring a 95% conversion yield of oleic acid.

2 Experimental

2.1 Synthesis of functionalized mesoporous carbon

Mesoporous carbon catalysts were synthesized by a soft-template method similar to the process described in previous works [10, 11]; as illustrated in Fig. S1. In summary, phloroglucinol (Sigma–Aldrich) and Pluronic F127 in the proportion of 1:1 (w/w) were dissolved in 30 mL of ethanol and water solution in the proportion of 10:9 (w/w) and kept under magnetic stirring at room temperature until diluted. HCl (0.48 mL) was added as a catalyst for the polymerization reaction. After 30 min, the solution turned light pink. Then, 7.5 mL of formaldehyde was added to this solution. The mixture was sonicated using an ultrasonic processor (Sonics & Materials, INC, model VC 505) operating at 20 kHz and equipped with a high-intensity solid titanium probe. The amplitude of the ultrasonic waves ranged from 20 to 80% (with an ON for 2 s and OFF for 1 s duty cycle). The time of exposure to ultrasound ranged from 15 to 60 min. The formation of a resin was observed, which was separated from the liquid phase and kept overnight in the hood.

The sample was heat treated in a Thermo Scientific tube oven using the following temperature program. The temperature was increased from room temperature to 180 °C (with a heating rate of 2 °C min^{-1}) and maintained at 180 °C for 5 am. Then, the temperature was increased from 180 to 400 °C (with a heating rate of 2 °C min^{-1}). Immediately after reaching 400 °C, it was increased to the final temperature (500 or 600 °C) using a heating rate of 5 °C min^{-1}. The material was kept at the final temperature for 2 h and subsequently allowed to cool to room temperature.

The carbon sample was functionalized in the proportion of 1 g of sample for 10 mL of concentrated sulfuric acid under magnetic stirring at 100 °C for 2 h to 8 h. The mixture was then filtered and washed with distilled water until no sulfate ions were present, which was detected with $BaCl_2$ solution. Finally, the sample was dried at 100 °C for 12 h.

The sulfonated catalyst samples were named MCSx-y, where MC represents the mesoporous carbon, x represents the carbonization temperature variation (400, 500 and 600 °C) and y is related to the sulfonation time. The term S is included only after sulfonation, and the term (R) is related to the catalyst recycled by four reaction cycles. For example, MCS5-4-R is the nomenclature for the mesoporous carbon sample carbonized at 500 °C, functionalized with sulfuric acid for 4 h and reused in four reaction cycles.

2.2 Characterization of functionalized mesoporous carbon

Scanning electron microscope (SEM) images were obtained by Vega 3, Tescan coupled to an energy dispersive X-ray spectroscopy system (EDS; INCA energy, United Kingdom). Fourier transform infrared spectrometer (FT-IR; Cary 630, Agilent) were determined in transmittance mode in the scanning range 4000–650 cm^{-1}. Thermogravimetric analysis (TG; TGA Q500, Shimadzu) was performed in the range from ambient temperature up to 850 °C with a heating rate of 10 °C min^{-1} and nitrogen flow of 100 mL min^{-1}. X-ray photoelectron spectroscopy measurements (XPS; VSW HA-100) used Al Kα radiation (hv = 1486.6 eV). The curve fitting was performed using Gaussian modeling, and the pressure during measurements was kept below 6×10^{-8} mbar. The density of acid sites on the catalyst was determined by the acid–base titration method using an NaOH 0.05 M solution and phenolphthalein as an indicator, as reported by Araujo et al. [12]. Nitrogen adsorption–desorption isotherms measured at − 196 °C using a volumetric analyzer (Belsorp Max, MicrotracBel Corp.). Nonsulfonated samples were heat treated at 200 °C for 2 h, while the sulfonated samples were heat treated at 120 °C for 2 h. The specific surface area was calculated by the Brunauer–Emmett–Teller (BET) method based on adsorption data in the relative pressure range of 0.05–0.15 p/p_0. The pore size distribution was calculated by the Barrett–Joyner–Halenda (BJH) model and the total pore volume (V_t) was estimated by the amount of nitrogen adsorbed at a relative pressure p/p_0 of 0.99.

2.3 Application of the catalyst in an acid catalyzed reaction

Esterification of oleic acid and methanol was selected as the test reaction. The catalytic experiments were carried out in a high-pressure benchtop reactor (mini Compact 5500 model, Parr Instrument Company). Esterification was carried out under the following conditions: a 12:1 methanol and oleic acid molar ratio and 5% catalyst loading at 100 °C for 1 h. At the end of the reaction, the solid catalyst was separated from the reaction medium by filtration, and the liquid phase was heated to 120 °C to remove the byproducts (methanol and water) from the mixture. The recovered catalyst was washed with n-hexane three times, dried at 100 °C for 12 h and reused in the next cycle of the reaction. After each reaction, the acid number of oleic acid and the product methyl oleate were calculated according to the AOCS 5a-40 standard, and the conversion of oleic acid was determined according to the European standard method EN 14.103 [13].

3 Results and discussion

3.1 Influence of ultrasound amplitude and time on mesoporous carbon preparation

The polymerization of phloroglucinol with formaldehyde was accelerated by treatment with ultrasound irradiation. Phloroglucinol was chosen because it has three highly reactive hydroxyl groups capable of forming covalent bonds to form a rigid polymeric structure [14]. The amplitude and time operating parameters were optimized to generate an pore structure. The influence of these two parameters was investigated using SEM and N_2 adsorption–desorption techniques (see Figs. 1, 2).

The SEM images (Fig. 1a) show that the mesoporous carbon samples obtained with an amplitude of 20% for 1 h (MC20%) have a smooth surface and small pores (macropores). Increasing the amplitude to 40% (MC40%) favored the enlargement of the structure's pores. When using an amplitude of 60% (MC60%), a surface with pores of different sizes that were well diffused was observed. In the range of 80% (MC80%), there is an irregular smooth surface and the appearance of a greater number of smaller pores. Samples MC40%, MC60% and MC80% fully polymerized in 30 min under ultrasonic irradiation.

The formation of pores on the catalyst surface was confirmed with surface area, pore size distribution and pore volume data calculated from N_2 adsorption–desorption isotherms (Fig. 1b). A hierarchical pore structure was found, that is, with micropores, mesopores and macropores in all carbon samples studied here. According to the IUPAC classification, the isotherms are of type IVa with hysteresis of type H1, reflecting the mesoporous structure found for the synthesized carbon materials. The isotherm presented a very accentuated inflection at the relative pressure p/p_0 0.77, indicative of capillary condensation inside uniform pores of cylindrical geometry [15, 16].

In the desorption isotherm, the capillary evaporation phenomenon did not present a delay in the evaporation of liquid nitrogen, indicating that there is no impediment to the exit of this gas, that is, that the cylindrical pore does not present a bottleneck. A slight increase in the amount of nitrogen (approximately 100 $cm^3\ g^{-1}$ STP) adsorbed at a relative pressure below p/p_0 0.1 was also observed, suggesting the presence of micropores in the pore structure. The contribution of micropores to the total volume was 11.5, 13.7, 17.5 and 19.6% for samples MC20, MC40, MC60 and MC80%, respectively; the volume of micropores remained within the expected range for mesoporous carbon synthesized by soft templates.

There was a decrease in the contribution of mesopores to the total volume from 88.5, 86.3, 82.5 and 80.4% for

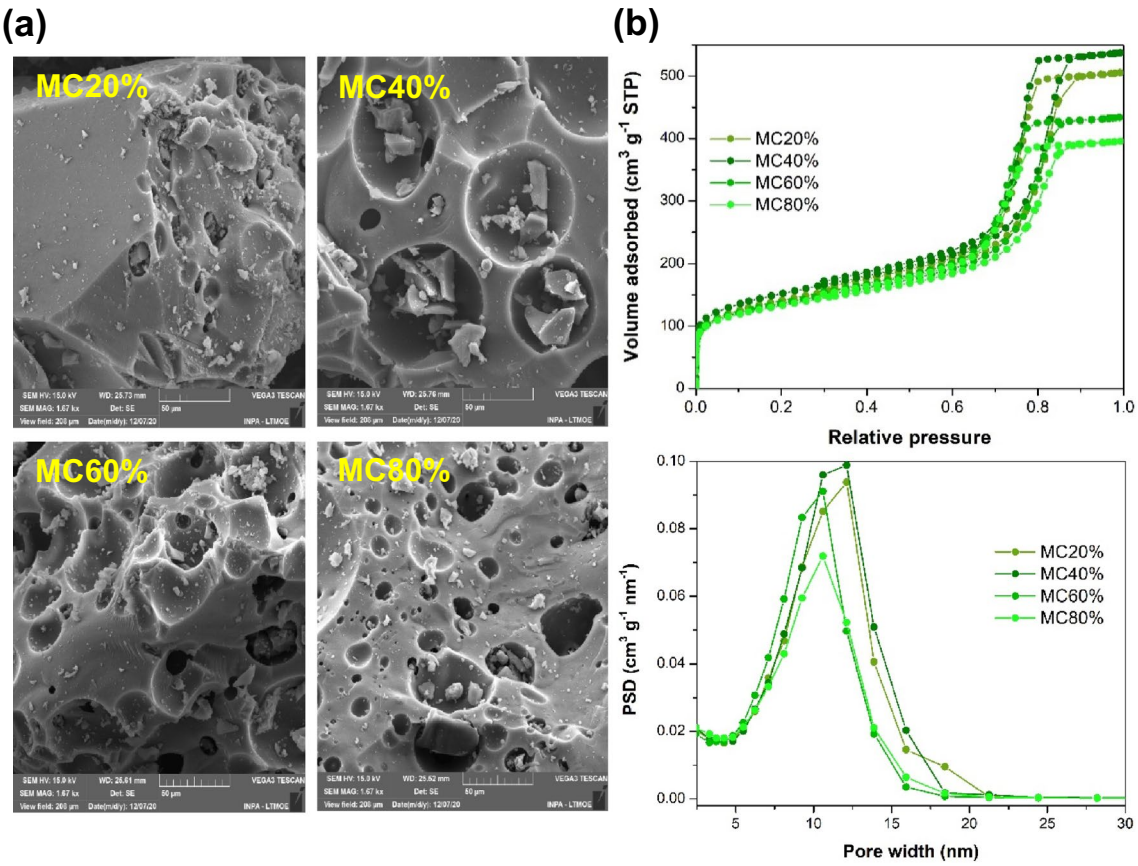

Fig. 1 Effect of ultrasonic amplitude variation on mesoporous carbon preparation. **a** SEM images and **b** N_2 adsorption–desorption isotherms and pore size distribution by the BJH method

samples MC20, MC40, MC60 and MC80%, respectively. The PSD curves illustrate a uniform mesopore size centered at 12 nm with a slight offset for smaller pore sizes; this is in agreement with the H1-type hysteresis, which is presented for materials with narrow uniform mesopore sizes.

The adsorption parameters calculated for the catalysts studied are shown in Table 1. The increase in amplitude caused a slight decrease in the surface area, going from 549 $m^2\ g^{-1}$ to 480 $m^2\ g^{-1}$ for samples MC40 and MC80%, respectively. The volume of mesopores decreased from 0.73 $cm^3\ g^{-1}$ (MC40%) to 0.51 $cm^3\ g^{-1}$ (MC80%), proving that an amplitude above 60% does not favor the formation of mesopores. Thus, the sample with 40% amplitude submitted for 1 h of sonication obtained better adsorption parameters and was chosen for the study of the variation in the synthesis time.

At synthesis times of 15 min and 60 min, insignificant variation was observed in the surface morphology of the samples (Fig. 2a) considering that the polymerization had already reached equilibrium after 30 min of ultrasonic irradiation. All samples of carbon materials shown in Fig. 2a exhibited irregular smooth surface morphology and a predominance of macropores. The samples named MC15min, MC30min, MC45min and MC60min present a hierarchical structure of pores containing micropores, mesopores and macropores.

With increasing ultrasonication time, the surface area increased from 500 $m^2\ g^{-1}$ (MC15min) to 549 $m^2\ g^{-1}$ (MC60min), while the increase in mesopore volume was negligible. The best adsorption parameters were found for the MC60min sample, prepared at an amplitude of 40%.

Amplitude is the most important parameter to be evaluated because it controls the amount of energy transmitted to the chemical reaction [17]. From the conversion of electrical energy into vibrating mechanical energy by the probe, pressure waves are created on the liquid, generating an alternating series of compression and rarefaction in the reaction medium. Successive series of this phenomenon generate cavitation bubbles that expand in the rarefaction phase and implode in compression. After reaching a critical point, the cavitation bubbles collapse releasing large amounts of energy in nanoseconds. It is estimated that the temperature can reach around 5,000 k with pressure at the moment of

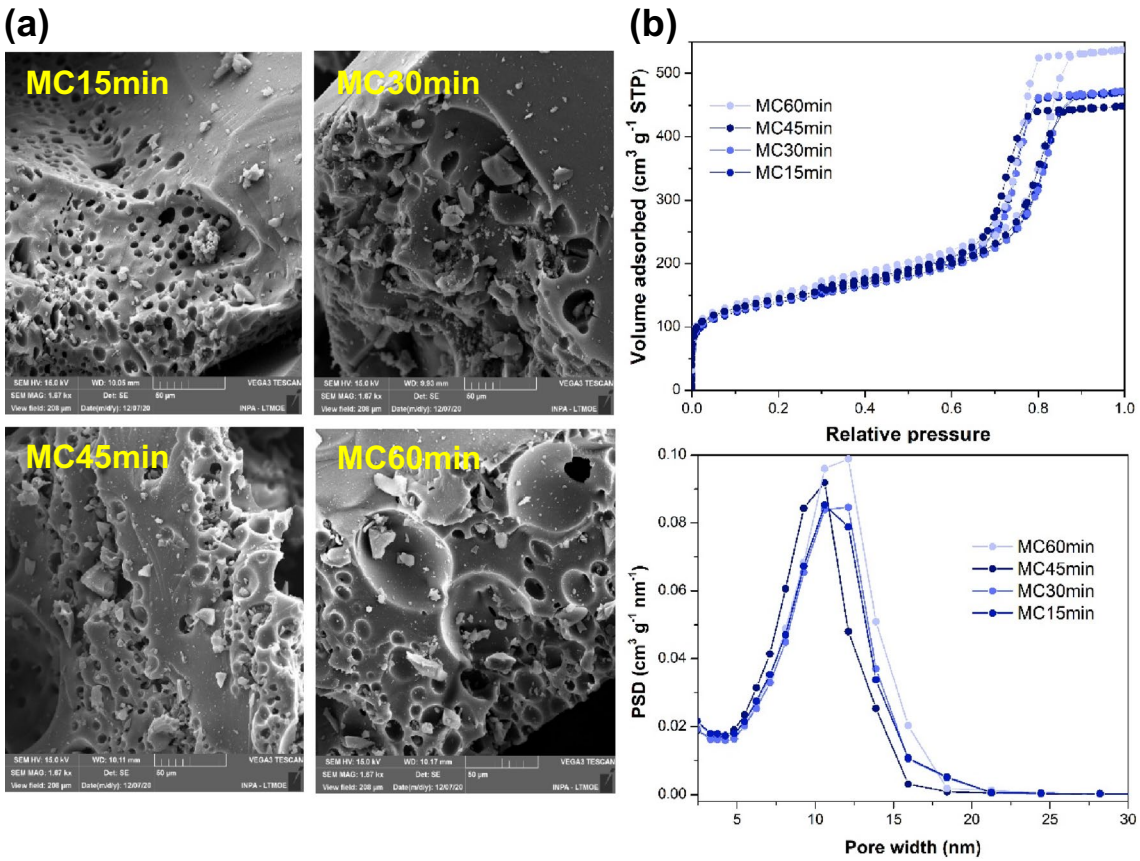

Fig. 2 Effect of ultrasonic time variation on mesoporous carbon preparation. **a** SEM images and **b** N_2 adsorption–desorption isotherms and pore size distribution by BJH

Table 1 Texture parameters determined by N_2 adsorption–desorption of mesoporous carbon materials synthesized under different conditions

Carbon	S_{BET}	V_t	V_{mi}	V_{me}	W_e
MC20%	505	0.78	0.09	0.69	12.1
MC40%	549	0.83	0.10	0.73	12.1
MC60%	494	0.67	0.10	0.57	10.6
MC80%	480	0.61	0.10	0.51	10.6
MC60min	549	0.83	0.10	0.73	12.1
MC45min	524	0.69	0.11	0.59	10.6
MC30min	510	0.73	0.10	0.63	12.1
MC15min	500	0.73	0.10	0.60	10.6
MC4	544	0.73	0.10	0.63	10.6
MC5	549	0.83	0.10	0.73	12.1
MC6	557	0.69	0.13	0.56	10.6
MC7	495	0.71	0.09	0.62	9.3
MC9	298	0.57	0.02	0.55	9.3

S_{BET} surface area ($m^2\ g^{-1}$), V_t single point pore volume ($cm^3\ g^{-1}$), $V_{mi} = V_t$-V_{me}–volume of micropores, V_{me}–volume of mesopores ($cm^3\ g^{-1}$), w_e mesopore (nm) width at the PSD maximum

collapse of 2,000 atm. The high pressures and temperatures cause the structure to rupture and the organization of new structures [18, 19].

3.2 Influence of carbonization temperature and functionalization with H_2SO_4 in the preparation of mesoporous carbon

The mesoporous carbon sample prepared in a range of 40% for 1 h (MC40%) was carbonized at temperatures from 400 to 900 °C, to evaluate the influence of temperature on the development of the hierarchical structure. According to the data extracted from the N_2 adsorption–desorption isotherms (Fig. 3), all isotherms remain of type IVa indicative of the presence of a hierarchical structure of micropores and mesopores (see Table 1).

The increase in the heat treatment temperature favored the destruction of the mesoporous structure, making it more rigid. A substantial decrease in surface area was achieved reaching a loss of 54% loss at a temperature of 900 °C. While the micropore and mesopore volumes remain practically constant. The pore size distribution followed the same trend described for the surface area decreasing with up to the pore size of 9.3 nm for the carbon sample treated at 900 °C. The heat treatment of the polymeric resin at temperatures above

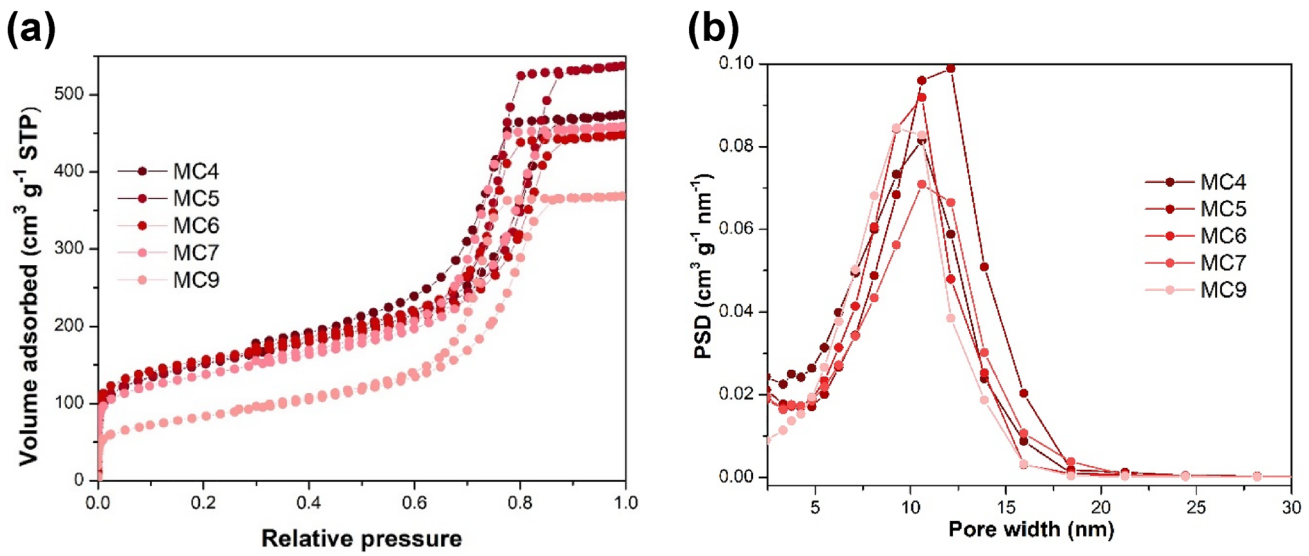

Fig. 3 Effect of carbonization temperature on mesoporous carbon preparation. **a** N_2 adsorption–desorption isotherms and **b** pore size distribution by BJH

600 °C favors the destruction pore ordering, as observed by Tang et al. [20].

The SEM images of mesoporous carbon at different carbonization temperatures (Fig. 4a) are an indication of the presence of micropores and mesopores. Thus, the carbonization temperature of 500 °C was chosen as ideal for preparing the samples of sulfonated mesoporous carbon catalysts. It is known that the presence of micropores favors high surface areas while the presence of mesopores enhances the mass transfer hampered by the microporous nature of

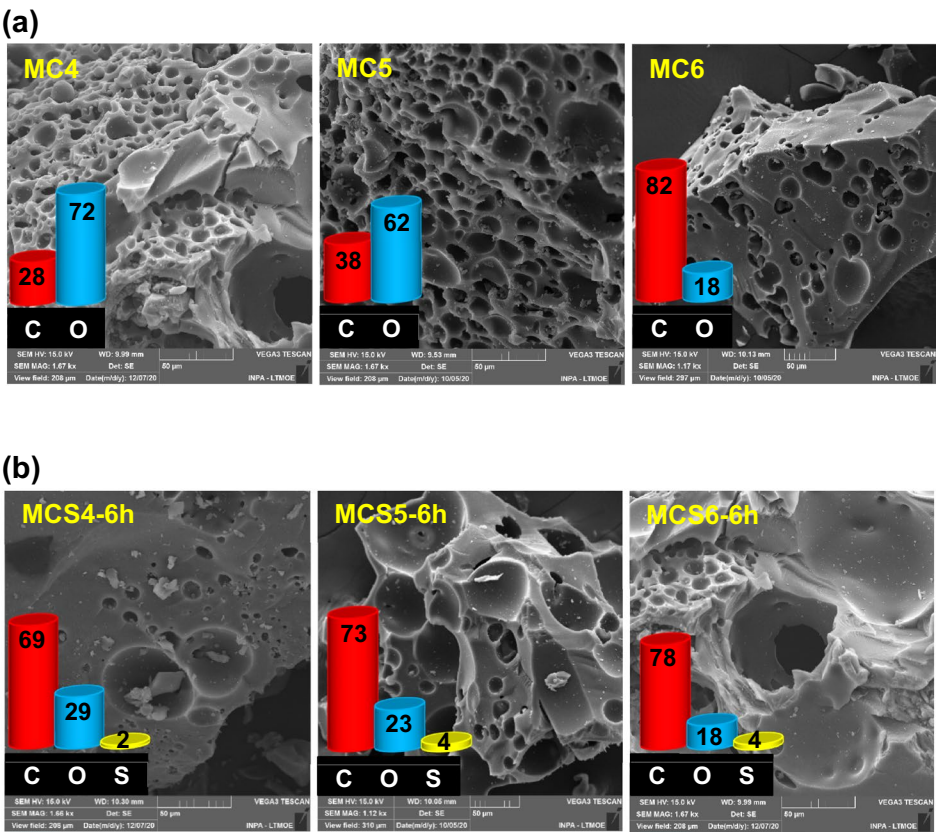

Fig. 4 SEM images of mesoporous carbon samples **a** before sulfonation and **b** after sulfonation

carbon materials in catalytic reactions [21]. However, its use in catalysis depends on functionalization with acid groups, that is, its catalytic activity results from the density of Brønsted acid sites [14].

Knowing this, the mesoporous carbon prepared in ultrasound was functionalized with acidic groups, preserving the mesoporous structure. After functionalization, the surface morphology changed (Fig. 4b), indicating a certain deformation caused by the attack of sulfuric acid.

Regarding the chemical composition of the catalysts, the EDS analysis (Fig. 4b) confirmed the signals of C, O and S in samples MCS4-6 h, MCS5-6 h and MCS6-6 h. Samples MC4 and MC5 have a higher composition of oxygen than carbon, while in sample MC6 the opposite happens due to the high temperature at which it was treated. After functionalization with sulfuric acid, the amount of carbon increased and the amount of oxygen decreased. Sulfur was added to the sulfonated samples, confirming the effectiveness of the functionalization method in anchoring the —SO_3H group to the surface of the mesoporous carbon, moreover, the results prove the acidic nature of the catalyst and are in agreement with the results of XPS and FT-IR.

The MCS4-6 h sample showed the greatest change in surface morphology, described as smooth and with few pores. This observation was confirmed by the analysis of N_2 adsorption (Fig. 5 and Table 2), which shows the surface area not exceeding 1 $m^2\ g^{-1}$ and negligible total volume, indicating the total loss of the mesoporous structure. Based on the esterification reaction yield values described in Table 2, it became clear that the activity of the MCS4-6 h catalyst on the esterification of oleic acid depended on the density of the sulfonic groups, and was shown to be independent of the textural properties studied here [14, 22].

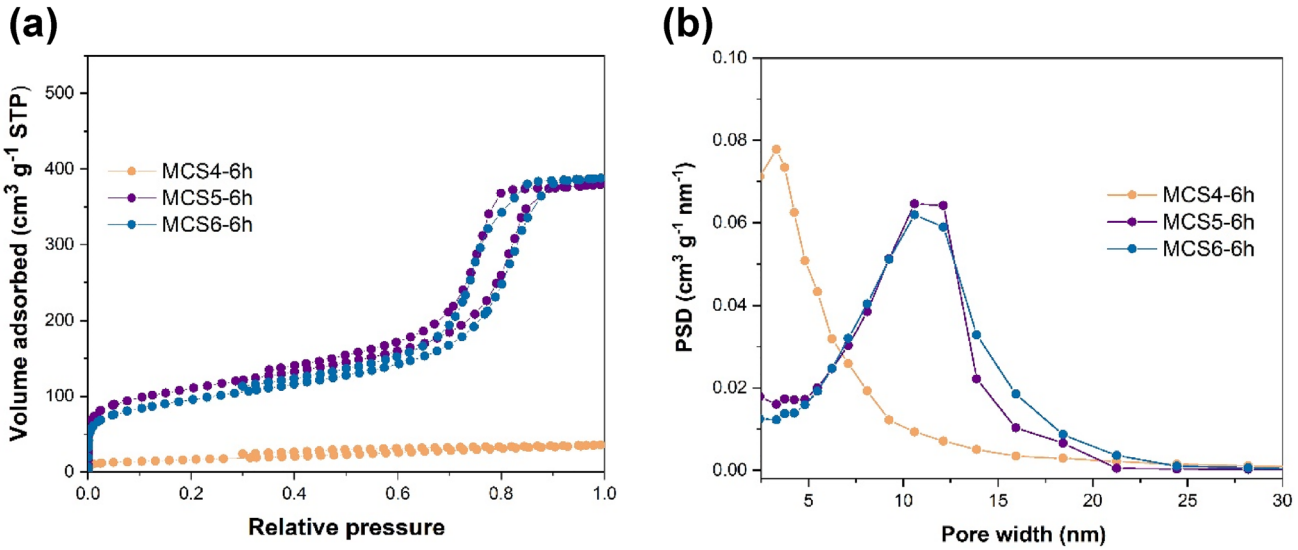

Fig. 5 Effect of sulfonation in the preparation of mesoporous carbon acid catalyst. **a** N_2 adsorption–desorption isotherms and **b** pore size distribution by BJH

Table 2 Texture parameters and catalytic activity of mesoporous carbon acid catalysts

Carbon	S_{BET}	V_t	V_{mi}	V_{me}	W_e	Acid density	Conversion (%)
MCS4-6 h	58	0.06	0.02	0.04	3.3	0.9	75
MCS5-4 h	364	0.58	0.07	0.52	10.6	1.0	80
MCS5-6 h	402	0.59	0.07	0.51	10.6	1.6	95
MCS5-8 h	295	0.46	0.05	0.41	10.6	2.3	92
MCS6-4 h	344	0.57	0.04	0.53	10.6	1.7	94
MCS6-6 h	343	0.60	0.05	0.55	10.6	1.5	93
MCS6-8 h	365	0.58	0.09	0.49	10.6	1.4	88

S_{BET} surface area ($m^2\ g^{-1}$), V_t single point pore volume ($cm^3\ g^{-1}$), $V_{mi} = V_t - V_{me}$–volume of micropores; V_{me}–volume of mesopores ($cm^3\ g^{-1}$), w_e mesopore (nm) width at the PSD maximum, acid density (mmol g-1)

The carbonization at 500 °C (MCS5-6 h) showed better surface area result (Fig. 5a) with a reduction of only 26% in the surface area value compared to the heat treated sample at 400 °C. The conversion of oleic acid reached a maximum of 95% for MCS5-6 h. This can be attributed to the small variation in textural properties, which contributed to a better interaction between pores and active sites during oleic acid adsorption. On the one hand, for the MCS6-6 h sample, the reduction was even greater, reaching 38% surface area loss (MC6 had a surface area of 557 $m^2\ g^{-1}$, and, after sulfonation, it had 343 $m^2\ g^{-1}$).

All samples remained with almost 87% porosity in the mesopore range (Fig. 5b) and the ordering of the mesopores was still maintained as shown in the TEM images (Fig. 8b). Despite the effects on textural parameters caused by the functionalization, the results presented here are superior to other solid acid catalysts such as Amberlyst-15, Nafion NR50 and $H_3PW_{12}O_{40}$ and mesoporous silicas [23].

3.2 Influence of sulfonation time on mesoporous carbon preparation

The catalyst carbonized at 400 °C (MCS4-6 h) had its textural properties drastically reduced after functionalization with H_2SO_4 and, therefore, the study of the variation of the sulfonation time was carried out only in the samples carbonized at 500 and 600 °C. Samples MCS5-6 h and MCS6-6 h converted oleic acid into ester by up to 95% (Table 2), maintaining a mesoporous structure.

The success in the sulfonation step is observed in the results of the N_2 adsorption–desorption isotherms (Fig. 6) and in the esterification reaction yield values (Table 2). Increasing the sulfonation time from 4 to 8 h did not significantly alter the textural properties of the catalysts (Fig. 6a-b). However, the MCS5-4 h sample showed a small decrease in oleic acid conversion (80%) compared to the MCS5-6 h sample (95%). The sulfonic group density of the MCS5-4 h sample was only 1.0 mmol g^{-1}, which may be due to its smaller surface area. This suggests that the reduction in conversion was due to a combination of surface area impacts (364 $m^2\ g^{-1}$) and acid site density [24].

It was observed that the sulfonation of mesoporous carbon for 8 h did not preserve the mesoporous structure, verified by the decay in the value of the surface area to 295 $m^2\ g^{-1}$ (MCS5-8 h). This change can be attributed to the relatively high content of acid groups introduced into the pore channels of the carbon structure, since the density of the sulfonic groups increased from 1.6 mmol g^{-1} (MCS5-6 h) to 2.3 mmol g^{-1} (MCS5-8 h) [2]. In this case, the reaction yield was favored by the density of the sulfonic groups. For samples MCS6-4 h, MCS6-6 h and MCS6-8 h (Fig. 6b), there was no significant variation in the textural parameter data summarized in Table 2.

Based on the results, the conversion of oleic acid into ester by the samples treated with sulfuric acid at 100 °C for 6 h (MCS5-6 h and MCS6-6 h) was slightly higher than the others. It should be considered that increasing the sulfonation temperature to 120 °C did not favor the results presented in Table 2. Furthermore, the use of higher temperatures is not favorable for the costs of large-scale processes. The results found are in agreement with many works in the literature that report a significant decay of textural properties after acid treatment [25].

Thermogravimetric analysis of the carbonized catalysts at 500 and 600 °C was used to approximately estimate the level of functionalization of the material, taking into account the amounts of mass loss of the three phases during heating. The DTG curves of the sulfonated samples (see Fig. 7a, b) precisely show the temperature regions in which the maximum mass losses occurred. The first loss was in the range of 30 to 144 °C and was attributed to the desorption of water molecules. The second loss started at 170 °C and was caused by the decomposition of sulfonic groups. Subsequent mass loss occurs above 450 °C due to the breakage of polymeric bonds.

Note the absence of the second mass loss for the unsulfonated samples (MC5 and MC6). This is further confirmation of the elimination of sulfonic groups strongly bound to the surface of the catalyst at this temperature. The increasing order of mass loss for —SO_3H was 4.2 and 6.7% for samples MCS5-4 h and MCS5-6 h, respectively. For samples MCS6-4 h and MCS6-6 h, they were 5.7% and 8.6%, respectively. These values are in agreement with the results found for the density of sulfonic groups (Table 2) and XPS (Fig. 9). Insertion of the group —SO_3H for 6 h shifted the curve to higher temperatures (200 °C). According to the literature data, this is typical for sulfonated mesoporous carbon materials [2].

These results indicate that all catalysts synthesized here are thermally stable below 170 °C, suggesting that the material should not be subjected to temperatures above 170 °C to avoid compromising the yield of the esterification reaction. Similar results were found for acid catalysts of mesoporous polymers [23, 26].

To further confirm the existence of a mesoporous structure in the catalysts, MCS5-6 h and MCS6-6 h were characterized by TEM. The images of unsulfonated samples MC5 and MC6 (Fig. 8) exhibit porous morphology. After the sulfonation step, the structural organization was conserved for the MCS5-6 h sample, while, for MCS6-6 h, there was a small pore disorder. These observations are supported by the N_2 adsorption–desorption data (Fig. 6a, b). The remarkably high thermal stability of these materials synthesized by ultrasound needs to be highlighted, which proved to be superior to other mesoporous carbons synthesized by the traditional method, where significant structural shrinkage

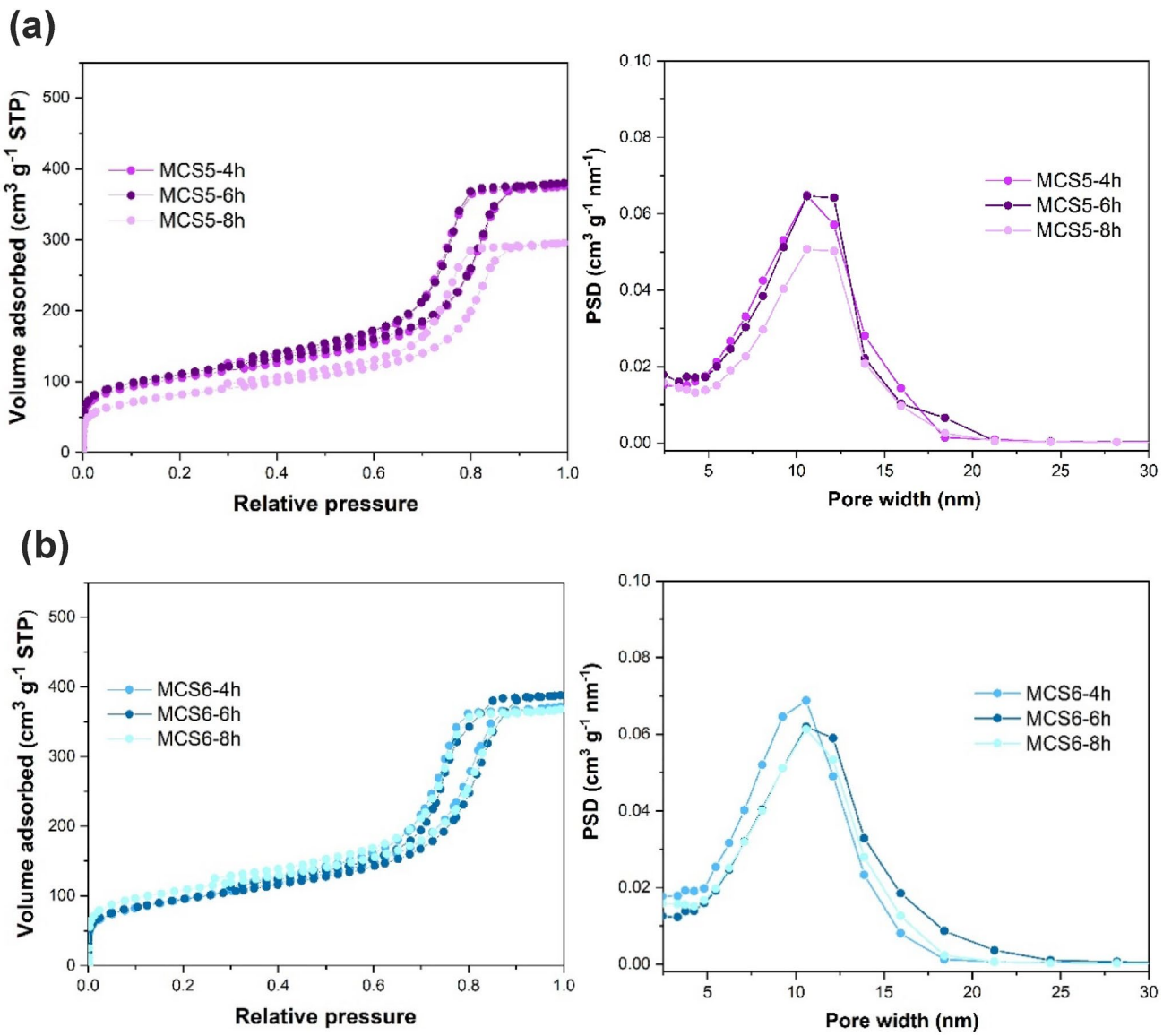

Fig. 6 N_2 adsorption–desorption isotherms and pore size distribution by the BJH method to analyze the effect of sulfonation time in the preparation of carbonized mesoporous carbon acid catalysts **a** 500 °C and **b** 600 °C

after treatment with acids and changes in textural properties were reported [15, 27].

The type of functional groups formed on the catalyst surface was determined by infrared spectroscopy. The FT-IR spectra of the sulfonated and nonsulfonated samples are shown in Fig. S2. Samples MC5, MC6, MCS5-6 h and MCS6-6 h have common absorption bands at 2345 cm^{-1} and 1580 cm^{-1} attributed to the C = C bond and at 1429 cm^{-1} related to the vibrational mode of the C–H bond, both present in the mesoporous carbon structure. The peak at 1157 cm^{-1} corresponds to the C–H and C–O–C asymmetrical vibrational stretching of the surfactant F127 [15]. The absorption band at 1698 cm^{-1} is attributed to the C = O bond present in the carboxylic acid (–COOH), which is indicative of the presence of acidic groups. The characteristic absorption peak of the C–S bond at 1038 cm^{-1} appeared after the sulfonation treatment, indicative of the presence of —SO_3H groups covalently linked to the carbon precursor structure [8].

The sulfonated samples MCS5-6 h and MCS6-6 h (Fig. 9) show peaks attributed to the signals of C1s, O1s and S2p characteristic of the presence of C, O and S in elemental form. The contents of C (75.1%), O (23.4%) and S (3.2%) are estimated. These results are in agreement with the EDS analysis (Fig. 4b).

The C1s spectra for all samples have in common the bond types C–C, C–O, C = O and O–C = O at binding energies at 284.5, 287, 288.9 and 290.8 eV, respectively (see spectra of

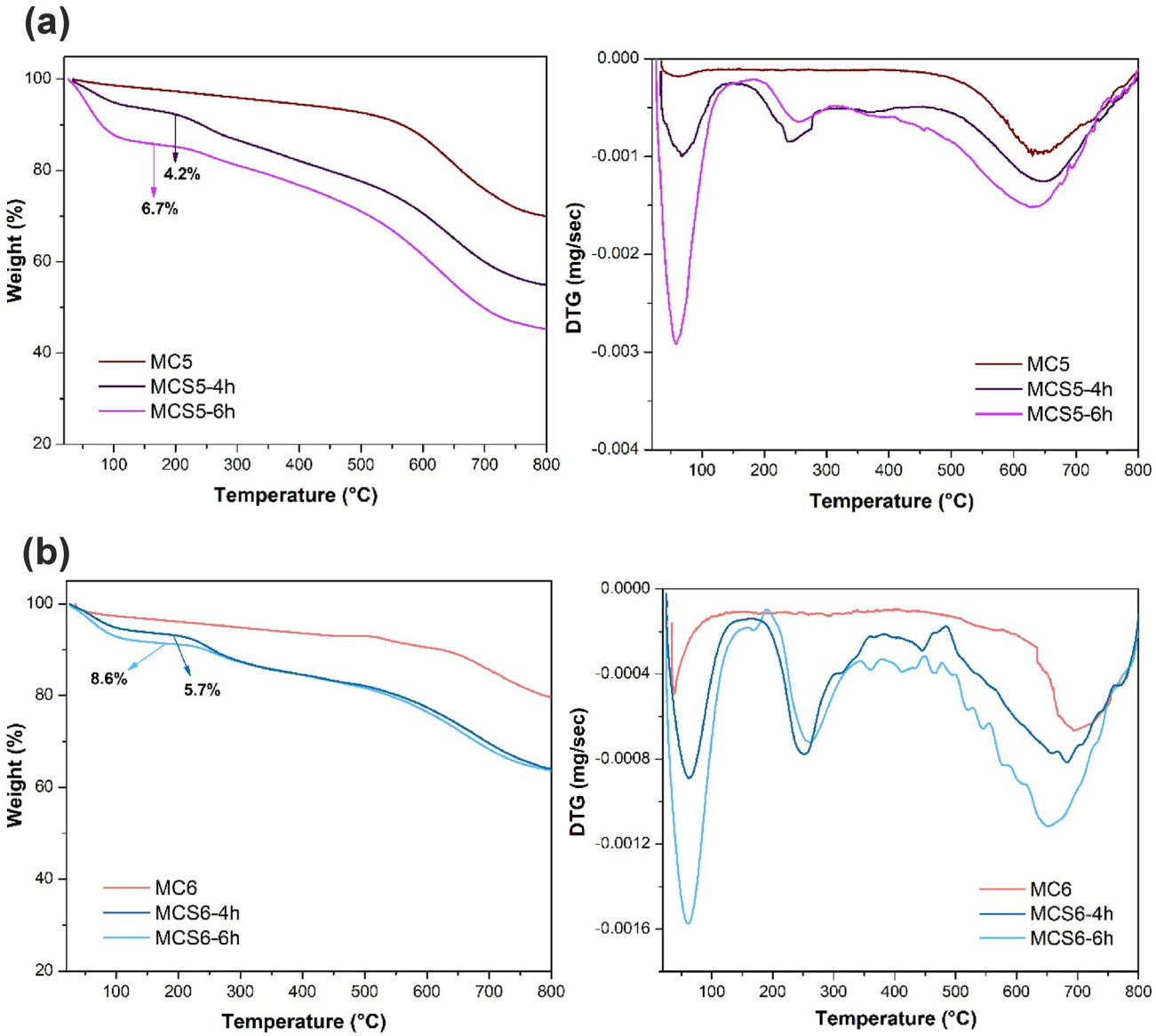

Fig. 7 TGA-DTG spectra to analyze the effect of sulfonation time on the preparation of the carbonized mesoporous carbon acid catalysts **a** 500 °C and **b** 600 °C

samples MC5 and MC6, Fig. S3). Sulfonated samples have an extra peak characteristic of the C–S bond at a binding energy of 285.8 eV [28]. The O1s spectra show three binding energy peaks of 530.3, 532.8 and 533.9 eV attributed to the C = O, C–O and O–H bonds, respectively. All bonds described above are typical of carbonaceous materials with polyaromatic surfaces [29].

The sulfonated samples differ from the nonsulfonated ones by the presence of sulfur. The $S2p_{3/2}$ peak at 167.8 eV represents the C–SO_2–C bond, and the $S2p_{1/2}$ peak at 168.9 eV is attributed to the C–SO_3–H bond. XPS results suggest that sulfur is present on the carbon surface primarily as sulfonic groups.

3.3 Optimized conditions for the conversion of oleic acid to methyl ester

In the present study, the maximum conversion of oleic acid was 95% in the MCS5-6 h sample. The results achieved were obtained under the following reaction conditions: a methanol and oleic acid molar ratio of 12:1 and a catalyst concentration of 5% by weight at 100 °C for 60 min. The study of the reuse of the MCS5-6 h catalyst was conducted under the conditions described above for five reaction cycles (see Fig. 10).

Sample MCS5-6 h exhibited relatively high catalytic efficiency (95% oleic acid conversion) and maintained

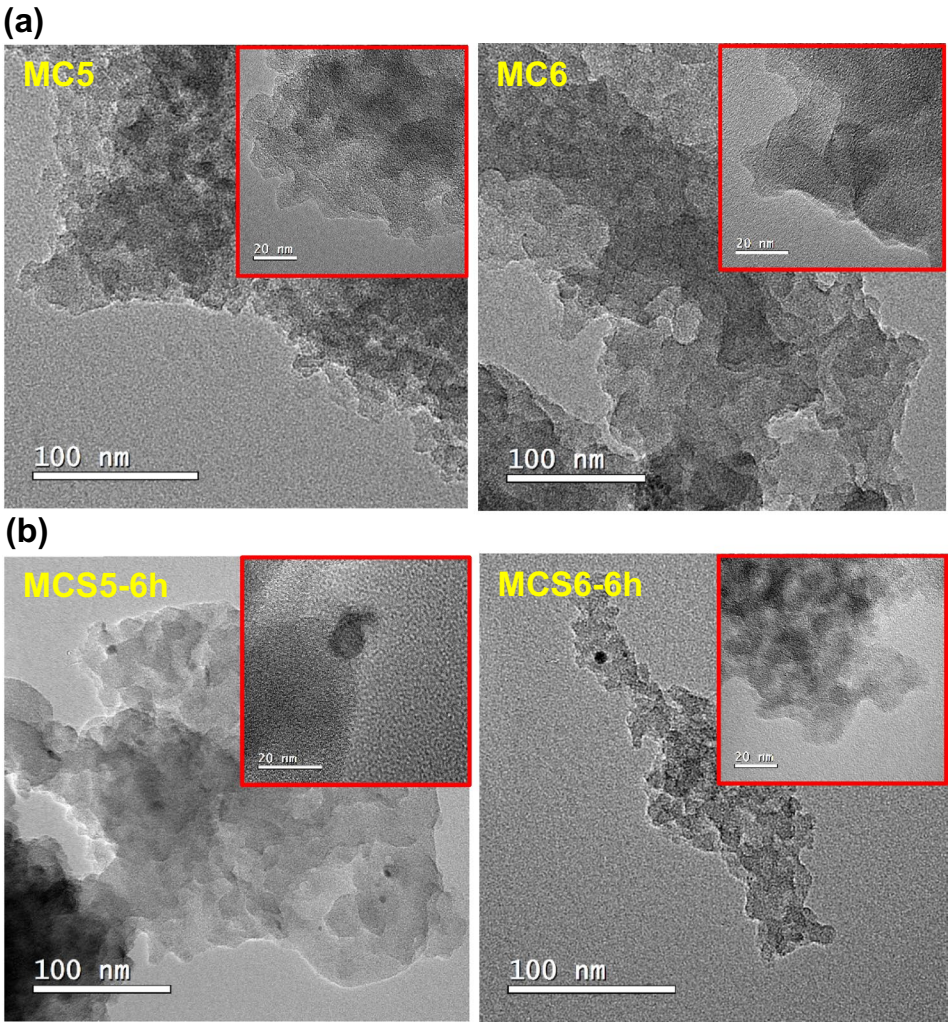

Fig. 8 TEM images of mesoporous carbon samples **a** before sulfonation and **b** after sulfonation

excellent quality catalytic activity after repeated use. The oleic acid conversion decreased by only 20% after continuous use until the fifth cycle. The main reason for this reduction is the combination of several factors, such as the leaching of active sites, as demonstrated by the decrease in the density of the —SO_3H group from 1.6 mmol g^{-1} in the first cycle to 0.61 mmol g^{-1} in the fifth cycle. The catalyst may also be deactivated due to pore blockage by impurities derived from the fatty acid and byproducts, although MCS5-6 h has sufficiently high porosity to minimize this effect [13].

Catalyst deactivation by leaching of the —SO_3H group was confirmed with FT-IR analysis (Fig. S4). The MCS5-6 h(R) spectrum shows that the band at 1038 cm^{-1} associated with C–S bonds is weaker after the fifth reaction cycle compared to the MCS5-6 h catalyst spectrum (Fig. S2). Overall, the results are promising for the application of mesoporous carbon catalysts synthesized by ultrasonic methods in reactions catalyzed by inorganic acids.

4 Conclusion

Mesoporous carbon was synthesized by the ultrasonic method with few synthesis steps and a short time period of 15 min at room temperature and atmospheric pressure. The efficiency of the process was governed by the amplitude and operating time of the equipment. The mesoporous materials maintained favorable physicochemical properties, i.e., high surface area, high pore volume and uniform pore size distribution. The MC5 sample showed superior textural properties, such as BET surface area (549 m^2 g^{-1}) and pore diameter (12.1 nm). The MCS5-6 h catalyst, with a sulfonic density of 1.6 mmol g^{-1}, BET surface area of 402 m^2 g^{-1} and pore diameter of 10.6 nm, remained mesoporous even after acid treatment. The MCS5-6 h catalyst showed excellent activity in the oleic acid esterification reaction with a 95% conversion yield under the optimized reaction conditions, which included a reaction time of 1 h at 100 °C, 5% by weight of catalyst and a molar ratio of oleic acid to methanol of 12:1. The recyclability of MCS5-6 h was five

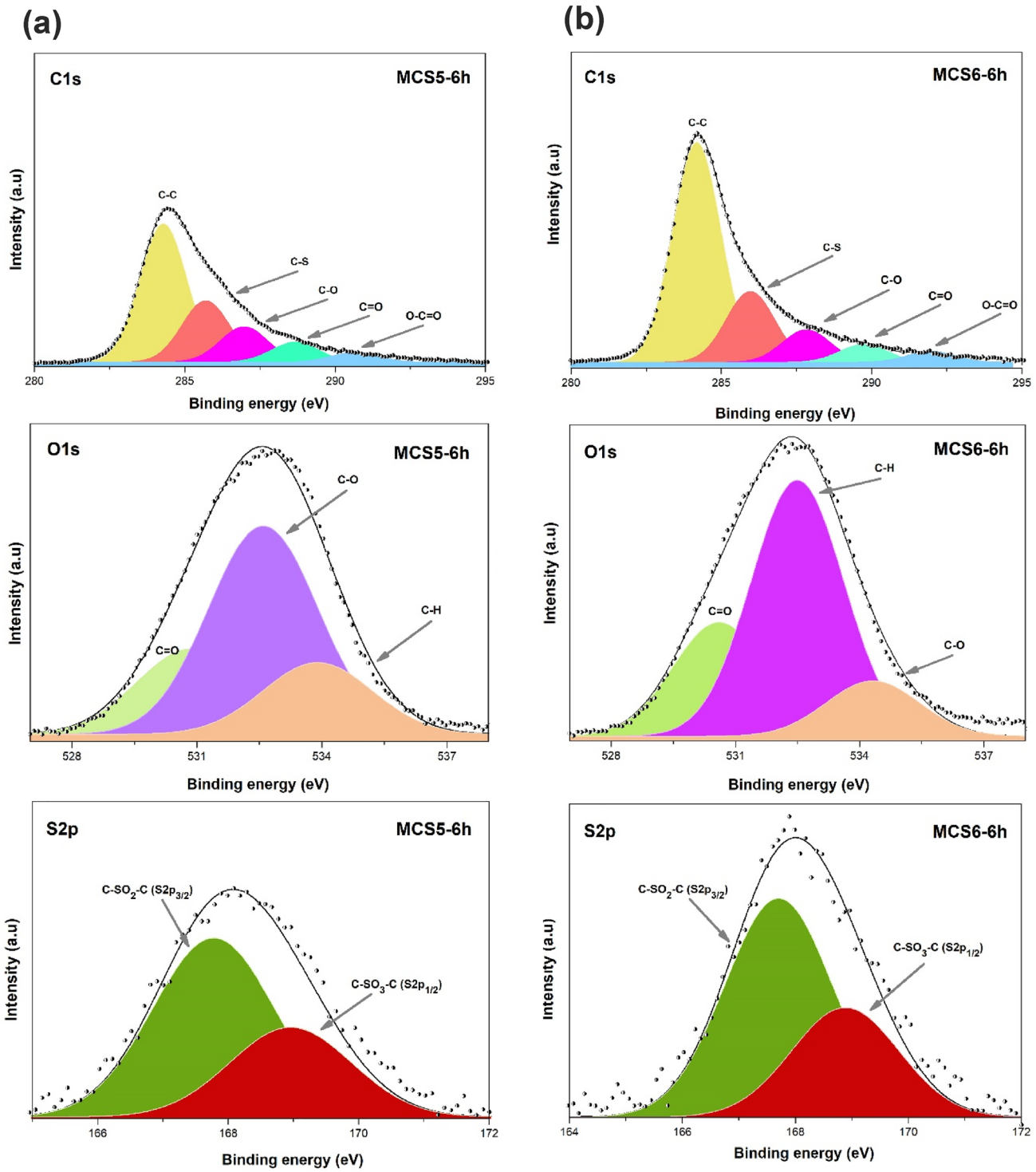

Fig. 9 XPS spectra of carbonized mesoporous carbon acid catalyst **a** 500 °C and **b** 600 °C

reaction cycles, showing a reduction of only 20% after the last cycle studied. In summary, the present work addressed a promising alternative for the synthesis of mesoporous carbon materials using ultrasound irradiation, thus providing an alternative with lower requirements of time and energy for large-scale production.

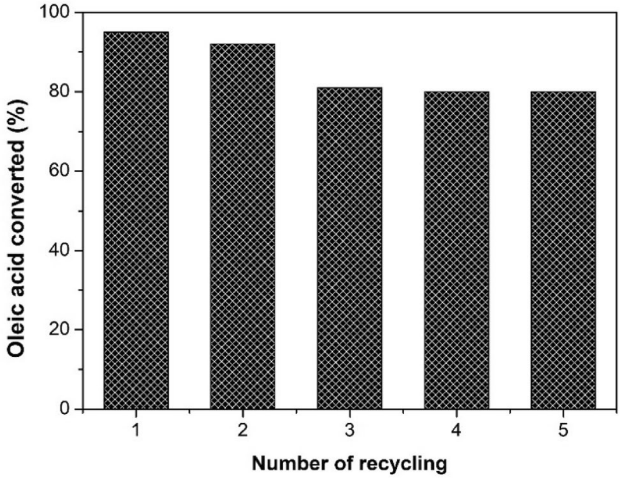

Fig. 10 Recycling of the MCS5-6 h(R) catalyst in the esterification reaction. Each reaction cycle was carried out under conditions of 5% catalyst loading and a molar ratio of oleic acid and methanol of 1:12 at 100 °C for 1 h

Supplementary Information The online version contains supplementary material available at https://doi.org/10.1007/s42823-022-00415-w.

Acknowledgements This work was financed by the Federal University of Amazonas and Amazonas State Research Support Foundation (FAPEAM)- Process N.° 01.02.016301.03414/2021-67, Edital N.° 010/2021- CT&I áreas prioritárias. This study was also financed in part by Coordenação de Aperfeiçoamento de Pessoal de Nível Superior - Finance Code 001.

Declarations

Conflict of interest We would like to declare that we have no known competing financial interests or personal relationships that could have appeared to influence the work reported in this paper.

References

1. Ashrafi S, Mousavi-Kamazani M, Zinatloo-Ajabshir S, Asghari A (2020) Novel sonochemical synthesis of Zn2V2O7 nanostructures for electrochemical hydrogen storage. Int J Hydrogen Energy 45(41):21611–21624. https://doi.org/10.1016/j.ijhydene.2020.05.166
2. Zailan Z, Tahir M, Jusoh M, Zakaria ZY (2021) A review of sulfonic group bearing porous carbon catalyst for biodiesel production. Renew Energy 175:430–452. https://doi.org/10.1016/j.renene.2021.05.030
3. Lee SK, Jo C, Kim J, Ryoo R (2020) Soft-to-hard consecutive templating one-pot route from metal nitrate/phenol resin/surfactant to mesoporous metal oxides with enhanced thermal stability. Microporous Mesoporous Mater 293:109767. https://doi.org/10.1016/j.micromeso.2019.109767
4. Zhou G, Yin J, Sun Z, Gao X, Zhu F, Zhao P, Li R, Xu J (2020) An ultrasonic assisted synthesis of rice-straw-based porous carbon with high performance symmetric supercapacitors. RSC Adv 10:3246–3255. https://doi.org/10.1039/C9RA08537H
5. El-Khodary SA, Abomohra AE-F, El-Enany GM, Aboalhassan AA, Ng DHL, Wang S, Lian J (2019) Sonochemical assisted fabrication of 3D hierarchical porous carbon for high-performance symmetric supercapacitor. UltrasonicsSonochemistry. 58:104617–104627. https://doi.org/10.1016/j.ultsonch.2019.104617
6. Ching TW, Haritos V, Tanksale A (2018) Ultrasound-assisted conversion of cellulose into hydrogel and functional carbon material. Cellulose 25:2629–2645. https://doi.org/10.1007/s10570-018-1746-y
7. Zhang K, Yao S, Li G, Hu Y (2015) One-step sonoelectrochemical fabrication of gold nanoparticle/carbon nanosheet hybrids for efficient surface-enhanced Raman scattering. Nanoscale 7(6):2659–2666. https://doi.org/10.1039/C4NR07082H
8. Tamborini LH, Militello MP, Balach J, Moyano JM, Barbero CA, Acevedo DF (2019) Application of sulfonated nanoporous carbons as acid catalysts for Fischer esterification reactions. Arab J Chem 12:3172–3182. https://doi.org/10.1016/j.arabjc.2015.08.018
9. Dong XQ, Jiang Y, Shan WB, Zhang M (2016) A novel highly ordered mesoporous carbon-based solid acid for synthesis of bisphenol-A. RSC Adv 6:17118–17124. https://doi.org/10.1039/c5ra24966j
10. Górka J, Zawislak A, Choma J, Jaroniec M (2010) Adsorption and structural properties of soft-templated mesoporous carbons obtained by carbonization at different temperatures and KOH activation. Appl Surf Sci 256(17):5187–5190. https://doi.org/10.1016/j.apsusc.2009.12.092
11. de Souza LK, Wickramaratne NP, Ello AS, Costa MJ, da Costa CE, Jaroniec M (2013) Enhancement of CO2 adsorption on phenolic resin-based mesoporous carbons by KOH activation. Carbon 65:334–340. https://doi.org/10.1016/j.carbon.2013.08.034
12. Araujo RO, da Silva CJ, Queiroz LS, da Rocha FGN, da Costa CEF, da Silva GC, de Souza LK (2019) Low temperature sulfonation of acai stone biomass derived carbons as acid catalysts for esterification reactions. Energy Convers Manag 196:821–830. https://doi.org/10.1016/j.enconman.2019.06.059
13. Araujo RO, Santos VO, Ribeiro FC, Chaar JDS, Falcão NP, de Souza LK (2021) One-step synthesis of a heterogeneous catalyst by the hydrothermal carbonization of acai seed. React Kinet Mech Catal 134(1):199–220. https://doi.org/10.1007/s11144-021-02059-9
14. Miao L, Zhu D, Zhao Y, Liu M, Duan H, Xiong W, Gan L (2017) Design of carbon materials with ultramicro-, supermicro-and mesopores using solvent-and self-template strategy for supercapacitors. Microporous Mesoporous Mater 253:1–9. https://doi.org/10.1016/j.micromeso.2017.06.032
15. Hegde V, Pandit P, Rananaware P, Brahmkhatri VP (2022) Sulfonic acid-functionalized mesoporous silica catalyst with different morphology for biodiesel production. Front Chem Sci Eng. https://doi.org/10.1007/s11705-021-2133-z
16. Wang H, Zhang W, Bai P, Xu L (2020) Ultrasound-assisted transformation from waste biomass to efficient carbon-based metal-free pH-universal oxygen reduction reaction electrocatalysts. Ultrason Sonochem 65:105048. https://doi.org/10.1016/j.ultsonch.2020.105048
17. Islam MH, Paul MT, Burheim OS, Pollet BG (2019) Recent developments in the sonoelectrochemical synthesis of nanomaterials. Ultrason Sonochem 59:104711. https://doi.org/10.1016/j.ultsonch.2019.104711
18. Perera CO, Alzahrani MAJ (2021) Ultrasound as a pre-treatment for extraction of bioactive compounds and food safety: a review. LWT 142:111114. https://doi.org/10.1016/j.lwt.2021.111114
19. Parthiban V, Bhuvaneshwari B, Karthikeyan J, Murugan P, Sahu AK (2019) Fluorine-enriched mesoporous carbon as efficient oxygen reduction catalyst: understanding the defects in porous matrix and fuel cell applications. Nanoscale AdV. 1(12):4926–4937

20. Tang X, Niu S, Zhao S, Zhang X, Li X, Yu H, Han K (2019) Synthesis of sulfonated catalyst from bituminous coal to catalyze esterification for biodiesel production with promoted mechanism analysis. J Ind Eng Chem 77:432–440. https://doi.org/10.1016/j.jiec.2019.05.008
21. Peer M, Qajar A, Rajagopalan R, Foley HC (2014) Synthesis of carbon with bimodal porosity by simultaneous polymerization of furfuryl alcohol and phloroglucinol. Microporous Mesoporous Mater 196:235–242. https://doi.org/10.1016/j.micromeso.2014.05.020
22. Laskar IB, Rajkumari K, Gupta R, Rokhum L (2018) Acid-functionalized mesoporous polymer-catalyzed acetalization of glycerol to solketal, a potential fuel additive under solvent-free conditions. Energy Fuels 32(12):12567–12576. https://doi.org/10.1021/acs.energyfuels.8b02948
23. Pan H, Li H, Zhang H, Wang A, Yang S (2019) Acidic ionic liquid-functionalized mesoporous melamine-formaldehyde polymer as heterogeneous catalyst for biodiesel production. Fuel 239:886–895. https://doi.org/10.1016/j.fuel.2018.11.093
24. Na S, Minhua Z, Xiuqin D, Lingtao W (2019) Preparation of sulfonated ordered mesoporous carbon catalyst and its catalytic performance for esterification of free fatty acids in waste cooking oils. RSC Adv 9:15941–15948. https://doi.org/10.1039/c9ra02546d
25. Soltani S, Rashid U, Yunus R, Taufiq-Yap YH (2016) Biodiesel production in the presence of sulfonated mesoporous $ZnAl_2O_4$ catalyst via esterification of palm fatty acid distillate (PFAD). Fuel 178:253–262. https://doi.org/10.1016/j.fuel.2016.03.059
26. Kanakikodi KS, Churipard SR, Halgeri AB, Maradur SP (2020) Solid acid catalyzed carboxymethylation of bio-derived alcohols: an efficient process for the synthesis of alkyl methyl carbonates. Representante Científico 10:13103–13115. https://doi.org/10.1038/s41598-020-69989-7
27. Bakhtiari B, Najafi Chermahini A, Babaei Z (2021) Design of an acidic sulfonated mesoporous carbon catalyst for the synthesis of butyl levulinate from levulinic acid. Environ Prog Sustainable Energy 40(6):e13721. https://doi.org/10.1002/ep.13721
28. Pan H, Li H, Liu XF, Zhang H, Yang KL, Huang S, Yang S (2016) Mesoporous polymeric solid acid as efficient catalyst for (trans) esterification of crude Jatropha curcas oil. Fuel Process Technol 150:50–57. https://doi.org/10.1016/j.fuproc.2016.04.035
29. Yang L, Yuan H, Wang S (2019) Preparation and application of ordered mesoporous carbon-based solid acid catalysts for transesterification and epoxidation. J Porous Mater 26:1435–1445. https://doi.org/10.1007/s10934-019-00742-w